Investigation of Adsorption Characteristics of Fibrinogen on Modified Gold Substrates Using Infrared Reflection Absorption Spectroscopy

Francis Nsiah [a] *, Mark T. McDermott [b]

[a]*Department of Chemistry, School of Physical Sciences, University of Cape Coast, Cape Coast, Ghana*
[b]*Department of Chemistry and National Institute for Nanotechnology*
University of Alberta, Edmonton, Alberta, Canada T6G 2G2
[a]*Email: fnsiah@ucc.edu.gh*
[b]*Email: mark.mcdermott@ualberta.ca*

Abstract

The adsorption characteristics of human fibrinogen (HFG) on surfaces with well-controlled chemistries have been studied using infrared reflection absorption spectroscopy. The surfaces examined in this study provide the experimental basis for exploring fundamental non-covalent intermolecular forces that dominate protein adsorption processes. Comparisons were drawn between fibrinogen and non-specifically adsorbed bovine IgG (bIgG) as well as structurally rigid lysozyme (LYS) on a positively-charged amine-modified surface to further understand substrate-influence on protein surface coverage. Work presented herein shows that surface coverage of an adsorbed protein depends largely on the nature of the substrate and the protein structure.

Keywords: Protein adsorption; Fibrinogen; Infrared reflection absorption spectroscopy; gold substrate**.**

1. Introduction

A comprehensive study of protein adsorption is highly desirable not only for gaining insight into the protein-surface interaction but also for predicting the possibility of using the surface for short- and long-term biomaterial applications.

----
* Corresponding author.

Interaction of proteins with solid surfaces and its related interfacial phenomena have been studied for decades [1-12]. A lot of effort has gone into understanding the adsorption-desorption kinetics [13] and conformational changes associated with adsorbed proteins on solid substrates [1, 3, 5, 14]. The desire to control and manipulate protein adsorption on surfaces therefore requires a detailed understanding of the adsorption process. Thus, protein adsorption characteristics are usually controlled by varying parameters such as surface chemistry, pH, ionic strength and substrate material [15, 16]. However, the effect of these factors on the activity of the surface-bound proteins has not been fully understood. It is generally accepted that protein adsorption and subsequent conformational changes are greatly influenced by surface hydrophobicity [2, 17-19]. The concomitant effect in the exposure of the interior hydrophobic groups drives attraction between neighboring adsorbed molecules.

Generally, adsorption of protein from solution to modified solid substrates is said to involve five processes [1, 3, 20, 21]. These include: (1) protein transport to the surface; (2) interaction and attachment to the surface; (3) adsorption; (4) structural and/or orientation rearrangements; and (5) desorption of the protein from the surface. Several techniques including atomic force microscopy (AFM) [22-24], surface plasmon resonance (SPR) [25], ellipsometry [26], radioactive labelling and infrared (IR) spectroscopy [27] have been employed to interrogate the adsorption behavior of proteins on surfaces. Although these techniques are powerful and provide valuable information on the state of the adsorbed protein, they are unable to distinguish between the individual protein molecules on the surface. For example, AFM has been used to observe the morphology and dynamic events of the adsorption process on a molecular scale [23, 24, 28], Surface topography of AFM provides information about the surface chemistry of the protein, which correlates to conformational changes and coverage of the adsorbed protein. However, tip contamination, damage of samples and imaging of weakly adsorbed molecules in liquid environment are challenges that need to be addressed. Also, measuring the rate of protein folding has remained elusive. Fourier transform infrared spectroscopy (FTIR) has been used to probe the conformational response of amide groups to changes in their environment which reflect possible changes in the whole protein structure [29-33]. The ability to provide distinct spectral signatures for proteins (amide bands) coupled with information on coverage and conformation response make infrared spectroscopy suitable for the work presented in this paper.

Among the numerous proteins investigated, fibrinogen has been studied most extensively due to its prominent role in coagulation and its ability to promote platelet adhesion [14, 24, 30, 34-38]. Fibrinogen is a massive dimeric protein (MW = 340kD) with several molecular domains. The structurally distinguishable regions of the fibrinogen molecule are: a lone central E domain, two distal D domains, two α-helical coiled coils, two αC domains, and a pair of junctions between them [34, 39]. At pH 7.4, the E and D domains are hydrophobic and negatively charged while the αC domain is hydrophilic and positively charged. Thus fibrinogen can interact with surfaces through a variety of mechanisms. For example, although, the overall charge of the molecule is negative ten (–10), a negative surface may adsorb through the αC domain [14]. Fibrinogen is therefore often referred to as a "sticky" protein due its ability to adsorb onto a variety of surfaces. The fibrinogen molecule has been found to exist in different possible orientations and/or conformations depending on the adsorption history and the surface chemistry of the substrate [14, 19, 34, 36, 40, 41]. Previous studies have shown that, following attachment to a surface, fibrinogen begins to increase its coverage in a manner consistent with unfolding on hydrophobic surfaces and reorientation on hydrophilic substrates [30,36]. This suggests that fibrinogen may

undergo either reversible or irreversible adsorption upon attachment depending on the substrate surface chemistry.

In the current study, the adsorption of HFG on neutral (polystyrene and 1-undecanethiol (UDT)), positively charged (11-amino-1-undecanethiol (AUT)) and negatively charged (11-mercapto-1-undecanoic acid (MUA)) surfaces was examined by infrared reflection absorption spectroscopy (IRRAS). Polystyrene modified and solution self-assembled thiol monolayer substrates were chosen to effect different surface interactions. Experiments conducted in this study were aimed at evaluating the effect of protein adsorption on solution self-assembled and adsorbed protein substrates. In the following sections, adsorbed protein substrates will be referred to as pre-HFG substrates. In all cases, protein concentrations were chosen to allow formation of a complete protein film after 1 h.

IRRAS has been used by our group and others to provide information on the adsorbed state of the protein and also as means of quantifying protein adsorption to the surfaces [4, 32, 33, 37, 40, 42]. Specifically, the intensity of amide II bands has been used to quantify the amount of protein present at the interface [33]. Also, peak shape analysis of amide I has also been applied to protein secondary structure or conformation [43]. Hence, in this study, the amide II band intensity will be used as a measure of amount of protein adsorbed to the substrate.

2. Materials and Methods

2.1. Reagents and materials

All aqueous solutions were prepared using water from a Nanopure (Barnstead, Dubuque, IA) purification system. Buffer solution employed salts from Fisher Scientific Company (Ottawa, ON). Phosphate buffered saline (PBS, pH 7.4) was prepared with reagent grade 1.4 mM KH_2PO_4 and 4.3 mM Na_2PO_4, 137 mM NaCl and 2.7 mM KCl. 1 mM PBS was used to prepare all protein solutions. All proteins were used as received without further purification. Fraction I 95% clottable human fibrinogen (HFG) was obtained from Sigma (St. Louis, MO). HFG solution concentrations were 14.7, 29.4, 58.8, 147, 294, 441 and 588 nM in 1 mM PBS. Bovine IgG (bIgG) was purchased from ICN Biomedicals (Aurora, Ohio) and diluted with PBS to achieve concentrations of 14.7 and 588 nM. Chicken lysozyme (LYS) was obtained from Sigma (St. Louis, MO) and prepared to concentrations of 14.7 and 588 nM.

1-undecanethiol ($HS(CH_2)_{10}CH_3$) (UDT) 98% and 11-mercapto-1-undecanoic acid ($HS(CH_2)_{10}COOH$) (MUA) 95% were purchased from Aldrich (Milwaukee, WI) and used as received. 11-amino-1-undecanethiol ($HS(CH_2)_{10}CH_2NH_2$) (AUT) was purchased from Dojindo Laboratories (Kumamoto, Japan). 1 mM thiol solutions were prepared in anhydrous ethanol (Quantum Chemical Co., Newark, NJ). Polystyrene (PS) was purchased from Aldrich (MW = 45,000 D), dissolved in tetrachloromethane (CCl_4) and 1 mM concentrations were prepared.

2.2. Substrate preparation

The glass substrates used were pre-cleaned in piranha solution (1:3 H_2O_2:H_2SO_4) at 90°C for 15 min, rinsed

several times with deionized water and dried with argon. All glass substrates used in this study were prepared by thermal evaporation of 15 nm adhesive layer of chromium and 200 nm of gold using a thermal evaporation system (Ion International Inc., New Windsor, NY). A vacuum of 4.6 x 10^{-6} mbar was used for evaporation at a rate of 0.2 Å/sec for Cr and 0.4 Å/sec for Au. Once prepared, the Au slides were rinsed using ethanol and water followed by drying with argon. The substrates were then cleaned in ozone cleaner (UVO-Cleaner, Model No. 42, Jelight Company Inc., Irvine, CA) for 10 min prior to immersion in thiol solution.

2.3. *Monolayer Formation and Substrate Modifications*

Self-assembled monolayers (SAMs) of UDT, MUA and AUT on Au for infrared reflection absorption spectroscopic studies were prepared from 1 mM ethanolic solutions. Only homogeneous single component monolayers were prepared. UDT and AUT were adsorbed overnight and MUA for 1 h. After the specified assembly time, the slides were removed from solution and rinsed well with ethanol to remove unbound thiols from the surface, and then dried with a stream of argon. A thin film of polystyrene was spin-coated onto gold slide using PWM32 Series Photoresist Spinner (Headway Research, Inc., Texas, USA). Protein films were formed by immersing the monolayer-modified Au slides in protein solution for 1 h. After the incubation period, the slides were removed from the protein solution, rinsed with 1 mM PBS to remove any unbound protein and dried with a stream of argon.
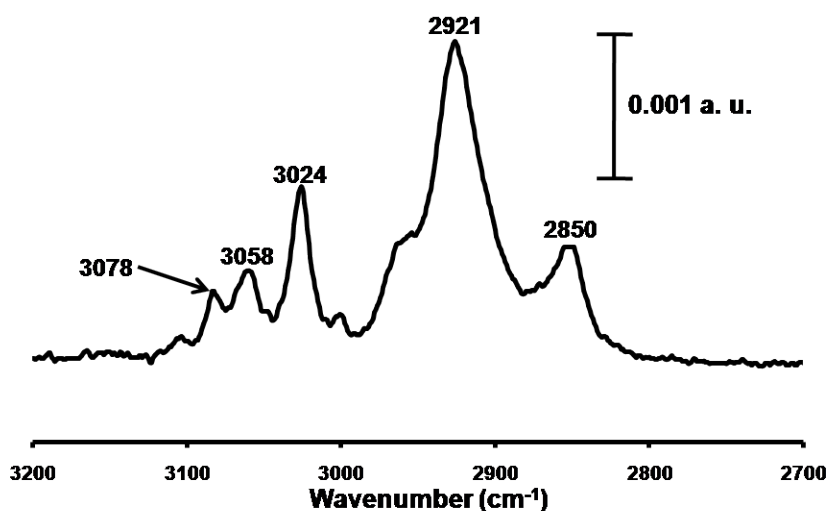

Figure 1: IRRAS spectrum of polystyrene on gold substrate. Bands shown are characteristic of C-H stretching modes for monosubstituted benzene ring and alkyl chain of the pol.

2.4 *Infrared spectra measurements*

IRRAS spectra were collected with a Mattson Infinity FTIR Spectrometer (Madison, WI) equipped with a low-noise mercury-cadmium-tellurium (MCT) detector cooled with liquid N_2 to about 77 K. A reflection accessory and a home-built sample holder housed in an external auxiliary bench were employed. Spectra for modified Au slides with UDT, MUA or AUT monolayer that has been immersed in HFG, LYS and IgG protein solutions

were collected. Protein adsorption on a thin film of polystyrene modified gold substrate was also studied. Spectra were taken at 2 cm^{-1} resolution with a glancing angle of 86° A self-assembled deuterated octadecanethiol was used as the background.

3. Results

The IRRAS characterization of polystyrene spin coated film on planar gold substrate is presented in Figure 1 whilst Figure 2 shows the C-H stretching frequencies of UDT, MUA and AUT self-assembled monolayers (SAMs) on planar gold substrates. Characteristic frequencies of these SAMs are indicated in Table 1.

Table 1: C-H stretching frequencies of UDT (HS(CH$_2$)$_{10}$CH$_3$), MUA (HS(CH$_2$)$_{10}$COOH), and AUT (HS(CH$_2$)$_{10}$CH$_2$NH$_2$) self-assembled monolayers on gold. n denotes the number of CH$_2$ units that make up the alkyl chain of the monolayer. ν_s and ν_a represent the symmetric and asymmetric stretches respectively. The ν_s(CH$_2$) and ν_a(CH$_2$) are respectively due to the symmetric and asymmetric C-H stretching modes of the CH$_2$ group of the alkyl chain. However, ν_s(CH$_3$) and ν_a(CH$_3$) are the symmetric and asymmetric C-H stretching modes of the CH$_3$ group which are present in UDT but absent in both MUA and AUT. N/A means not applicable.

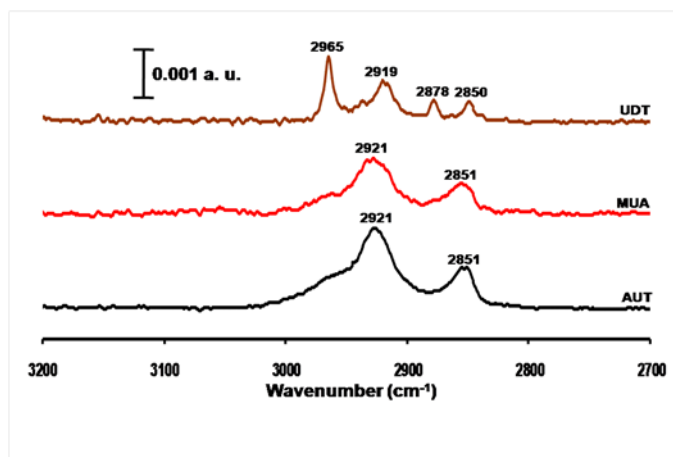| Number of Methylene Units (n)	Monolayer	ν_s(CH$_2$) (cm^{-1})	ν_a(CH$_2$) (cm^{-1})	ν_s(CH$_3$) (cm^{-1})	ν_aCH$_3$ (cm^{-1})
10	UDT	2850	2919	2878	2965
10	MUA	2851	2921	N/A	N/A
11	AUT	2851	2921	N/A	N/A

Figure 2: FTIR spectra of 1 mM solutions of self-assembled monolayers (SAMs) of UDT (CH$_3$-terminated), MUA (COOH-terminated) and AUT (NH$_2$-terminated) adsorbed on gold substrate. C-H stretching frequencies of UDT, MUA and AUT self-assembled monolayers on planar gold substrates are similar to those of polystyrene shown earlier.

Figure 3 and 4 respectively show the IRRAS spectra collected after 1 h adsorption of 14.7 and 588 nM HFG on polystyrene, UDT, MUA and AUT modified Au substrates. Spectroscopic measurements of 14.7 and 588 nM concentrations of fibrinogen (HFG) adsorbed on different gold substrates which are modified with UDT, MUA and AUT self-assembled monolayers (SAMs) are as shown in Table 2.
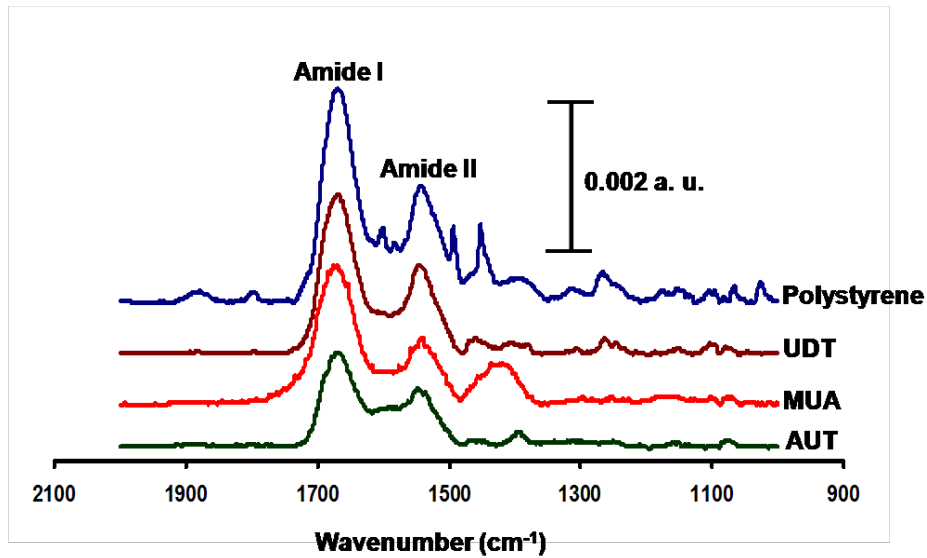

Figure 3: Spectra obtained following 1 h adsorption of 14.7 nM HFG onto polystyrene, UDT, MUA and AUT modified planar gold substrates. The presence of amide peaks in each spectrum indicates that HFG did adsorb to all these surfaces.
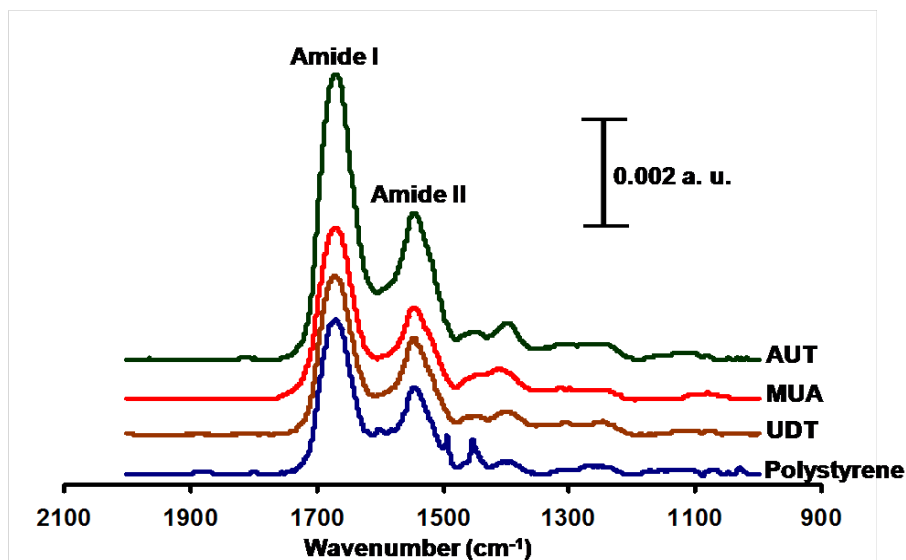

Figure 4: IRRAS investigation showing 1 h adsorption of 588 nM HFG on different chemistries of polystyrene, UDT, MUA and AUT modified planar gold substrates. Presence of amide bands indicates protein adsorption onto the substrates.

71

Table 2: Spectroscopic measurements of 14.7 and 588 nM concentrations of fibrinogen (HFG) adsorbed on different gold substrates which are modified with UDT, MUA and AUT self-assembled monolayers (SAMs). Adsorbed protein spectra were collected at resolution of 2 cm^{-1}. For band positions, the average value for 6 measurements is reported and the standard deviation of the average was lower than the resolution (2 cm^{-1}) of the measurement. Absorbance measurements shown are also average values and standard deviations of 6 spectral measurements.

HFG adsorbed on	Peak Position (cm^{-1})			Absorbance (a.u.)	
	Amide I	Amide II 14.7 nM	Amide II 588 nM	Amide II 14.7 nM	Amide II 588 nM
Polystyrene	1669 ± 1	1543 ± 1	1545 ± 1	0.00147 ± 0.00002	0.00368 ± 0.00003
UDT	1670 ± 1	1543 ± 1	1545 ± 1	0.00121 ± 0.00001	0.00382 ± 0.00002
MUA	1670 ± 1	1543 ± 1	1545 ± 1	0.00091 ± 0.00003	0.00365 ± 0.00002
AUT	1669 ± 1	1543 ± 1	1546 ± 1	0.00080 ± 0.00001	0.00548 ± 0.00001

Figure 5 presents the spectra of pre-formed HFG substrates on MUA SAM before and after exposure to PBS. IRRAS measurements of both 14.7 and 588 nM HFG before and after incubation in PBS are given in Table 3.

Table 3: Tabulated spectroscopic measurements for evaluation of binding strength of adsorbed 14.7 and 588 nM of fibrinogen (HFG) on MUA substrate. Amide II absorbance is a diagnostic indicator for the amount or coverage of adsorbed protein. For band positions, the average value for 3 measurements is reported and the standard deviation of the average was lower than the resolution (2 cm^{-1}) of the measurement. Absorbance measurements shown are also average values and standard deviations of 3 spectral measurements.

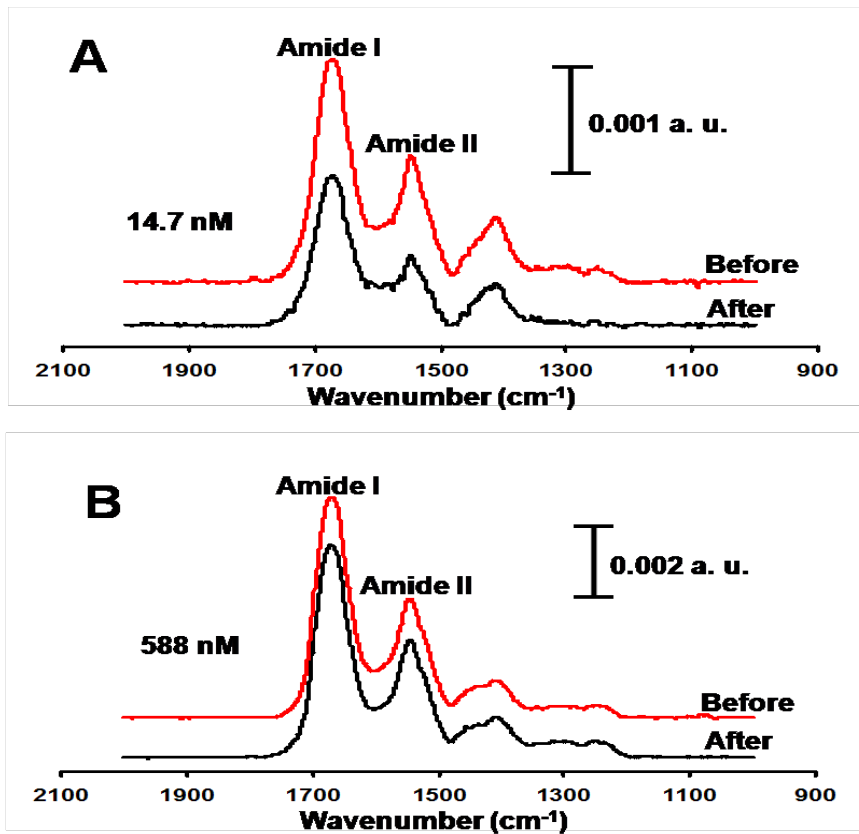| HFG adsorbed On MUA	Peak Position (cm^{-1})			Absorbance (a.u.)	
	Amide I	Amide II 14.7 nM	Amide II 588 nM	Amide II 14.7 nM	Amide II 588 nM
Before PBS	1670 ± 1	1543 ± 1	1545 ± 1	0.00088 ± 0.00002	0.00367 ± 0.00001
After 1 h in PBS	1671 ± 1	1540 ± 1	1545 ± 1	0.00067 ± 0.00002	0.003242 ± 0.00001
% Change (after – before)				24	12

Figure 5: Investigation of possible desorption of HFG from MUA substrate. (A) Spectra showing adsorbed 14.7 nM HFG on MUA substrate before and after PBS displacement. (B) Before and after 588 nM HFG desorption by PBS from MUA-derived substrate.
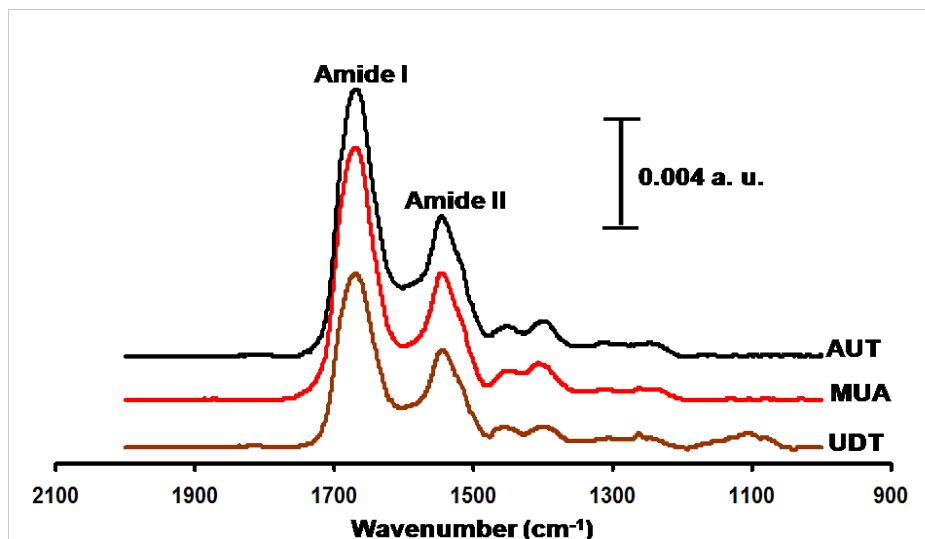

Figure 6: IRRAS spectra for 588 nM human fibrinogen (HFG) following 1 h adsorption time on 14.7 nM pre-HFG on planar gold substrates modified with AUT, MUA and UDT SAMs. The presence of amide peaks in each spectrum indicates that HFG did adsorb to all these surfaces.

73

Table 4: IRRAS measurements for 14.7 and 588 nM HFG adsorbed on the SAMs substrates with pre-formed HFG films. For band positions, the average value for 3 measurements is reported and the standard deviation of the average was lower than the resolution (2 cm^{-1}) of the measurement. Absorbance measurements shown are also average values and standard deviations of 3 spectral measurements.

Pre–HFG adsorbed on	Peak Position (cm^{-1})			Absorbance (a.u.)	
	Amide I	Amide II 14.7 nM	Amide II 588 nM	Amide II 14.7 nM	Amide II 588 nM
UDT	1670 ± 1	1543 ± 1	1546 ± 1	0.00125 ± 0.00001	0.00361 ± 0.00002
MUA	1670 ± 1	1544 ± 1	1546 ± 1	0.00095 ± 0.00002	0.00464 ± 0.00002
AUT	1669 ± 2	1544 ± 1	1546 ± 1	0.00080 ± 0.00001	0.00513 ± 0.00001

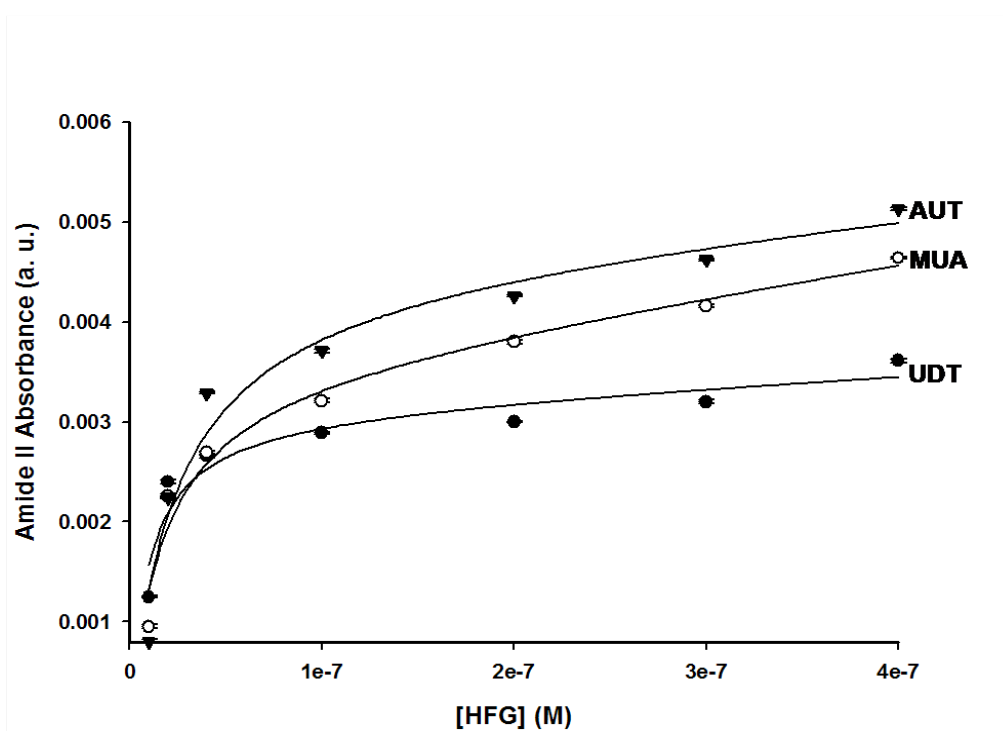**Figure 7:** Binding curve showing HFG coverage on pre-HFG gold substrates modified with different chemistries. Amide II absorbance was used as a measure of the amount of adsorbed protein on the surface of the various self-assembled monolayers. Solution concentrations of HFG track its surface coverage. Plots indicate HFG adsorption on UDT (filled circles), MUA (open circles) and AUT (filled triangles).

Table 5: Curve-fitting parameters for HFG curves for both SAM-modified and the pre-HFG substrates. The SAM substrates consisted of UDT, MUA and UDT self-assembled monolayer (SAM) chemistries.

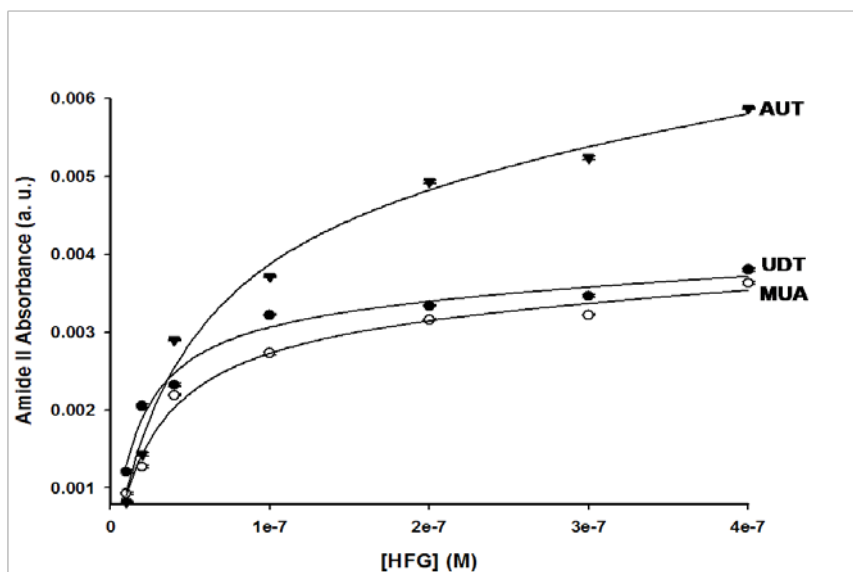| SAM	Substrate	B_{max}	K_{ads} (M^{-1})	R^2
UDT	SAM modified	$3.5\ (0.3) \times 10^{-3}$	$5.8\ (0.24) \times 10^{7}$	0.98
	Pre–HFG	$3.1\ (0.1) \times 10^{-3}$	$1.0\ (0.22) \times 10^{6}$	0.95
MUA	SAM modified	$3.5\ (0.2) \times 10^{-3}$	$3.6\ (0.14) \times 10^{7}$	0.99
	Pre–HFG	$3.5\ (0.2) \times 10^{-3}$	$5.7\ (0.15) \times 10^{7}$	0.97
AUT	SAM modified	$5.3\ (0.1) \times 10^{-3}$	$2.2\ (0.62) \times 10^{7}$	0.99
	Pre–HFG	$4.5\ (0.2) \times 10^{-3}$	$4.1\ (0.88) \times 10^{7}$	0.96

Figure 8: Binding curve showing HFG coverage on gold substrates modified with different chemistries. Amide II absorbance was used as a measure of the amount of adsorbed protein on the surface of the various self-assembled monolayers. Solution concentrations of HFG track its surface coverage. Plots indicate HFG adsorption on UDT (filled circles), MUA (open circles) and AUT (filled triangles).

4. Discussions

4.1 Surface Characterization

Characterization of a set of surfaces exhibiting systematic variations in surface chemistry is required to effectively determine chemical functionalities responsible for influencing protein adsorption to solid substrates. Infrared spectroscopy has been used in the past to probe the methylene C-H stretches of films formed on gold substrates [44-46]. For example, Porter *et al.* observed asymmetric CH_2 stretch at approximately 2918 cm^{-1} for long chain thiols, indicative of crystalline monolayer [44]. Shorter chain thiols exhibited a blue shift in their absorption energies. Therefore, IRRAS was employed in this study to ascertain the formation of spin-coated polystyrene film and solution self-assembled thiol monolayers of 1-undecanethiol, 11-mercapto-1-undecanoic acid and 11-amino-1-undecanethiol on gold. The C-H adsorption bands between 2700 and 3200 cm^{-1} spectral

region were monitored.

Figure 1 shows the infrared spectrum of polystyrene molecules that have been spin coated on a planar gold substrate. Spectral features at positions 3078, 3058 and 3024 cm^{-1} are characteristic C-H stretching modes for mono substituted benzene ring [47]. The presence of these bands indicates that polystyrene is immobilized onto the gold substrate. Bands at 2921 and 2850 cm^{-1} are the C-H stretching modes for the symmetric and asymmetric CH_2 groups respectively on the alkyl chain of the polymer. Molecular self-assembled techniques provide an effective means of fabricating organic surfaces with well-defined structure and chemistry. Spectra of Figure 2 were realized from substrates modified with 1-undecanethiol ($HS(CH_2)_{10}CH_3$,UDT), 11-mercapto-1-undecanoic acid ($HS(CH_2)_{10}COOH$, MUA) and 11-amino-1-undecanethiol($HS(CH_2)_{10}CH_2NH_2$, AUT). These thiols have different chemistries but similar number of methylene units. The CH_2 stretching mode adsorption intensity is directly related to the number of CH_2 units per alkyl group. Assignment of the bands for UDT, MUA and AUT in the C-H stretching region (high frequency region, 2700 to 3200 cm^{-1}) is indicated in Table 1. The C-H region describes the chain structure of the monolayer. All the characteristic bands of the monolayers are indicative of crystalline (highly-ordered) chain structures. The values shown in Table 1 are indications of relatively dense alkyl chains in crystalline-like environments and are in good agreement with literature results [44]. These SAMs were carefully chosen to eliminate the influence of the monolayer structure on the adsorption process whilst presenting varied surface chemistries for protein interaction.

Table 6: IRRAS measurements of the adsorption of HFG, IgG and LYS on AUT-patterned gold substrates. Amide I and amide II bands are used respectively as diagnostic indicators for conformational changes and as a measure of the amount or coverage of adsorbed proteins.

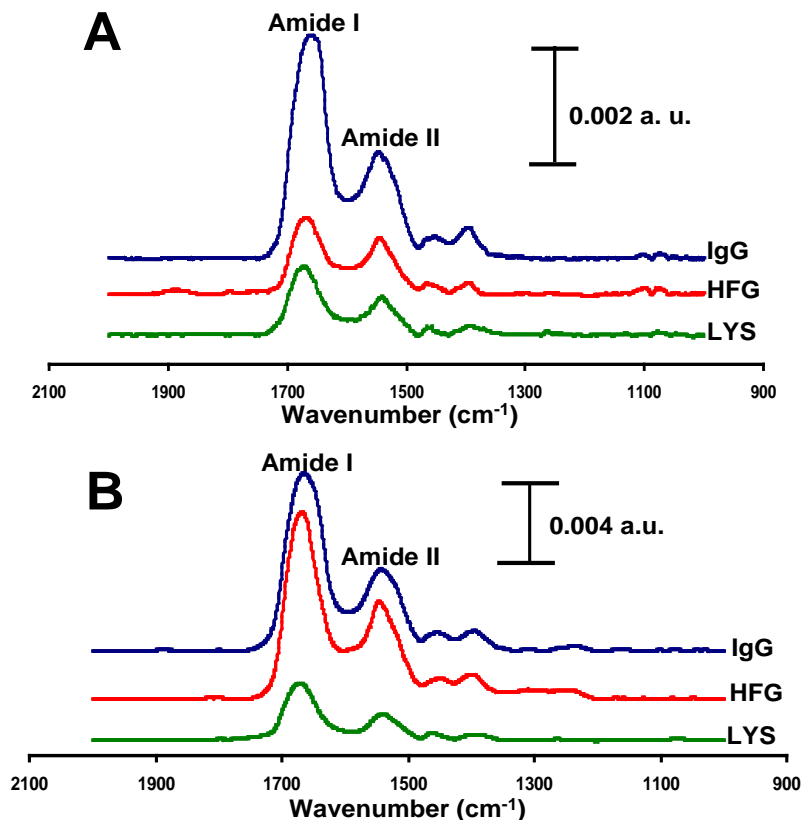| Adsorbed Protein on NH₂ Substrate	Peak Position (cm^{-1})			Absorbance (a.u.)	
	Amide I	Amide II 14.7 nM	Amide II 588 nM	Amide II 14.7 nM	Amide II 588 nM
HFG	1669 ± 2	1544 ± 1	1546 ± 1	0.00085 ± 0.00003	0.00583 ± 0.00001
Bovine	1662 ± 1	1545 ± 1	1543 ± 1	0.00183	0.00434
IgG				± 0.00001	± 0.00001
LYS	1670 ± 2	1540 ± 1	1540 ± 1	0.00068 ± 0.00002	0.00137 ± 0.00002

Figure 9: Comparison of adsorption characteristics of HFG, IgG and LYS adsorbed on AUT-patterned gold substrates. (A) IRRAS spectra of 14.7 nM LYS, HFG and bIgG after 1 h exposure time. (B) Similar experiment on AUT using concentrations of 588 nM solutions of the proteins in (A).

4.2 Adsorption of Human Fibrinogen on Modified Substrates

The discussion in the following section will focus on the effect of surface chemistry on adsorption characteristics of proteins on solid substrates. In all cases, protein concentrations were chosen to allow formation of a complete protein film after 1 h. IRRAS spectra from 2100 to 900 cm^{-1} of adsorbed proteins will be presented. In this spectral range, proteins and peptides exhibit characteristic bands, which are the direct results of vibrations in the amide linkages. The amide I band (C=O stretch) appears in the region from 1650 to 1680 cm^{-1} and the amide II band (combination of C-N stretch and N-H bend) is generally located at 1550 cm^{-1} [33, 48-50]. Amide I and amide II bands have been used respectively as diagnostic indicators for conformational changes and as a measure of the amount or coverage of adsorbed proteins [23, 48-50]. Amide III band in the vicinity of 1240 cm^{-1} resulting from N-H bending is weakly absorbing as compared to amide I and amide II. Hence no discussion on this band will be presented. The absorbance of the amide II band is linearly related to the amount of protein bound to the surface [51]. Thus, the intensities of amide II bands serve as useful indicators for protein coverage. Hence, amide II band intensity will be used in this study as a measure of amount of protein adsorbed to the substrate. In addition, adsorbed protein substrates will be referred to as pre-HFG substrates.

Figure 3 and 4 respectively show the IRRAS spectra collected after 1 h adsorption of 14.7 and 588 nM HFG on

polystyrene, UDT, MUA and AUT modified Au substrates. All substrates were rinsed with 1 mM PBS and dried with argon to remove any unbound protein prior to IRRAS analysis. These spectra show two strong absorbances corresponding to the amide I and amide II bands. Table 2 presents the summary of the infrared spectroscopic measurements of the amide bands in Figures 3 and 4. The differences observed in the amide I bands were less than our spectral resolution. In addition, the peak positions of amide II bands for adsorbed HFG on the four surfaces are very similar. This is not surprising since it has been shown that the amide II peak positions are insensitive to the adsorbed state of the protein [33]. The presence of amide bands indicates adsorption of fibrinogen on these different surface chemistries.

The spectra describing the adsorption of 14.7 and 588 nM HFG solutions on a polystyrene/Au substrate are shown in Figures 3 and 4 respectively. The presence of ring stretching modes from the polystyrene film is an indication of incomplete protein coverage at both concentrations within the 1 h adsorption time used in this study. Analysis of these spectra shows a similar pattern of HFG adsorption on polystyrene and UDT substrates at the two HFG concentrations studied. The methyl and polystyrene substrates are expected to retain significant hydrophobic character. As noted previously, it has been established by other groups that proteins denature to a greater extent on hydrophobic surfaces, a process that exposes interior hydrophobic groups and drives attraction between neighboring adsorbed molecules [4, 14, 52]. These results imply that HFG adsorbs in a similar fashion on the neutral polystyrene and UDT surfaces as confirmed by their surface HFG coverage shown in Table 2.

In Table 2, a close examination of amide II peak intensities of 14.7 nM fibrinogen on MUA and AUT charged surfaces following 1 h adsorption show similar protein coverage. The amide II absorbance for the AUT modified surface is 0.00080 a.u. compared to 0.00091 a.u. for the carboxyl-terminated surface. The data indicate almost equal affinity for protein adsorption on the positively charged AUT SAM surface and its counterpart negatively-charged MUA SAM at lower solution concentrations. In addition, these values may reflect electrostatic repulsion from oppositely charges surface species at lower solution concentrations. However, the amide II absorbance values measured on the AUT and MUA charged surfaces are lower than those recorded on both polystyrene and UDT hydrophobic surfaces. Higher quantities observed on polystyrene and UDT modified gold substrates at lower concentration might be a direct result of surface-induced conformation/orientation changes due to the high degree of protein denaturation on such surfaces. As noted previously, denaturation serves to maximize interaction between the hydrophobic surface groups leading to greater protein coverage [4, 33, 36, 53].

A sharp increase in the amide II absorbance is noted in Figure 4 after the adsorption of a 588 nM HFG solution on AUT-derived substrate. The amide II band is linearly related to the amount of protein bound to the surface [33, 51]. Thus, HFG adsorption on amine-modified gold substrate recorded the greatest protein surface coverage. Fibrinogen is a massive protein with regions of both negative and positive charges. The overall charge of the protein at physiological pH is -10 [14]. Therefore, this highest observed coverage might have resulted from the electrostatic interaction between the negatively charged E and D domains of the HFG molecule with the amine substrate. This result is consistent with that reported by Evans-Nguyen *et al.* on fibrinogen adsorption amine surfaces [35].

Finally, Figure 4 comparatively illustrates the amide II peak intensities following the 588 nM HFG adsorption on polystyrene, UDT and MUA. The amide II absorbances measured on these three surfaces are not statistically different (based on t-test at the 95% confidence level) at the higher HFG concentration. This suggests that HFG has similar coverage on these surfaces. However, HFG is expected to exhibit different conformations on these surfaces with different chemistries. For systems where electrostatic interactions play an important role, the maximum adsorption will be affected by charges from both adsorbate and the surface. Hence, the negatively charged fibrinogen molecule would experience electrostatic repulsion from the negatively charged carboxylate functionalities on the MUA substrate resulting in low protein coverage.

4.3 Desorption of Adsorbed Fibrinogen

It is expected that weaker electrostatic interaction would lead to more reversible interactions whilst hydrophobic effects would be largely responsible for irreversible protein adsorption. To ascertain this possibility, we investigated the possible fibrinogen desorption from the MUA-derived substrates using phosphate buffer at physiological pH. In order to investigate desorption and/or displacement of fibrinogen, and the influence of the underlying MUA monolayer, three sets of MUA-modified gold substrates were used. The substrates were simultaneously immersed in two sets of fibrinogen concentrations used in this study. After 1 h incubation period and thorough rinsing with PBS, three of the slides were analyzed using IRRAS. The other three slides were quickly transferred to freshly prepared 1 mM PBS solution, incubated for another 1 h and analyzed.

Figure 5 presents the spectra of pre-formed HFG substrates on MUA SAM before and after exposure to PBS. The positions of amide I and II bands recorded before and after 1 h exposure to PBS solution are very similar. This suggests that the adsorbed HFG is not perturbed by PBS solution. IRRAS measurements of both 14.7 and 588 nM HFG before and after incubation in PBS are given in Table 3. About 24% adsorbed HFG was displaced at lower concentration (Figure 5A) whereas only 12% was desorbed at higher concentration (Figure 5B). The significance of this result stems from a previous report which correlated the amount of fibrinogen eluted with sodium dodecyl sulfate with platelet binding [54]. HFG that was more tightly bound to polymer surfaces exhibited a lower affinity for platelets than a loosely bound layer. Hence, since interfacial platelet aggregation is a key step in the formation of a blood clot, the biocompatibility of a surface may be influenced by how tightly it binds fibrinogen. Again, looking at the relatively small amounts of adsorbed HFG displaced, it can be deduced that there is no single interaction responsible for fibrinogen adsorption on modified substrates.

4.4 HFG Adsorption onto Pre-HFG Substrates

In the following sections, the adsorption of human fibrinogen to substrates having pre-formed HFG films will be examined. Pre-formed HFG substrates will be referred to as pre-HFG substrates. The sequential adsorption experiment will allow us to probe the effect of a pre-formed protein layer on the adsorption of subsequent HFG and examine any displacement or co-adsorption processes. According to Oscarsson, the structures of underlying substrates do not only influence the protein-covering the layer but also the adsorption characteristics and subsequent binding to other protein molecules [55]. Hence, the objective of this particular study is to evaluate the influence of both SAM-modified and the pre-HFG substrates on subsequent HFG adsorption.

Figure 6 depicts the adsorption of 588 nM HFG onto 14.7 nM pre-HFG substrates with underlying AUT, MHA and UDT self-assembled monolayers as indicated. The spectral measurements are summarized in Table 4. Comparison between Figures 4 and 6 supply some interesting qualitative details about the state of adsorbed HFG at each functional group. First, the positions of the amide I bands of the adsorbed HFG to both SAM-modified and the pre-HFG substrates are very similar. This implies that the HFG molecule retains its conformation on the pre-HFG substrates at each functional group. Secondly, the amount of HFG adsorbed on pre-HFG substrate with underlying methyl functionality is comparable to its counterpart recorded in Table 2. This might reveal the exerted influence of the underlying methyl functionality on the adsorption pattern of HFG on both substrates. Thirdly, visual inspection of the pre-HFG substrates for both MUA and AUT films seems to show differences in coverage compared those shown in Table 2. However, statistical analysis shows no difference in the amount of HFG coverage for the two methods. In summary, the details of the spectral analysis in this study suggest that the amount of adsorbed HFG is mainly influenced by the underlying thiol monolayer chemistry with barely any contribution from the pre-adsorbed protein film.

4.5 Adsorption Isotherms of Fibrinogen on Modified Surfaces

The objective of this investigation is to use infrared spectroscopy to model the HFG binding to different substrates. FTIR has been shown to have sufficient sensitivity to be used for studying protein adsorption in both solution and on solid support [30, 31, 37, 56]. In the following section, the protein isotherms were constructed using substrates prepared in two different ways. The aim was to help further examine the influence of the SAM monolayer and that of the pre-formed protein film on the surface coverage of HFG.

First, single SAM modified substrate was exposed to various HFG solutions with concentrations ranging from 14.7 to 588 nM (as pre-HFG substrates). Substrates prepared this way mimic single channels that are widely employed to measure binding strengths of biological interactions [57]. The substrate was sequentially immersed in each solution for 1 h and IRRAS spectra were taken each time. The amide II bands spectral measurements on each substrate were recorded and plotted against each HFG solution concentration. Figure 7 shows adsorption isotherms constructed by plotting amide II absorbance for the pre-HFG substrates initially modified with UDT, MUA and AUT SAMs against various HFG solution concentrations. The binding constants of fibrinogen on the different substrates were determined by fitting the amount of HFG adsorbed (using amide II absorbance) to the range of solution concentrations using Langmuir-type equation given below:

$$y = \frac{B_{\max} K_{ads} x}{1 + K_{ads} x}$$

where y is the amount of protein adsorbed to the modified gold substrate, $B_{\max}$ is the adsorption capacity (maximum amount of protein adsorbed), $K_{\max}$ is the adsorption coefficient and x is protein solution concentration. When y = 0.5, the above equation can be solved for the solution concentration of adsorbate corresponding to half-maximal surface coverage. At this concentration, $x = K_{ads}^{-1}$, hence the value of the adsorption coefficient correspond to the inverse of the concentration at half-saturation coverage. The initial steep slopes of the plots shown in Figure 7 reflect high affinity of fibrinogen for the SAM-modified substrates. The amount adsorbed

levels off as the adsorption sites are gradually filled.

The second approach involved the use of different SAM modified substrates for different HFG concentrations. Figure 8 shows adsorption isotherms constructed by plotting amide II absorbance for HFG adsorbed on UDT, MUA and AUT modified substrates against various HFG solution concentrations. The AUT-derived substrate shows a steeper slope compared to both MUA and UDT derived substrates. The fitting parameters of the HFG binding curves are given in Table 5. Since the adsorption phenomena appeared to follow a typical Langmuir isotherm, K_{ads} can be estimated from the binding curves. K_{ads} is a measure of the binding strength of the complex formed between the protein and the substrate. For example, a large K_{ads} value indicates that the protein has a high binding affinity for the substrate.

Three observations are noteworthy from the adsorption isotherms presented in Figures 7 and 8. First, Figure 7 shows better correlation coefficient (R^2) values compared to those obtained from Figure 8, indicating a better agreement between the fit and the data. Secondly, the adsorption capacity (B_{max}) values obtained for the fits are very similar for all the plots. This implies that the recorded amide II intensities are not solely due to surface-protein interactions but rather a combination of nonspecific adsorption and specific binding. Thirdly, K_{ads} values determined from the Langmuir fit varies with surface chemistry. All the K_{ads} values presented in Table 5 for both methods are very similar (~10^7 M^{-1}), indicating that HFG has similar affinity towards all surfaces studied in this work. It must be noted that the distribution of hydrophobic and hydrophilic residues as well as charged groups on the protein surface are important determinants in protein complex formation on modified surfaces. These exposed surface functionalities predict the adsorption characteristics of the protein. As a rule, hydrophilic surfaces more weakly adsorb proteins than hydrophobic surfaces [1]. Our results do not clearly show any distinction based on K_{ads} for the different substrates. We might, in future, have to look at the affinity between immobilized anti-HFG and its HFG antigen at high HFG concentration to help address the effect of surface chemistry on protein coverage. However, FTIR-based adsorption studies provide an interesting quantitative evaluation of fibrinogen binding SAMs functionalized gold substrates in a label-free format.

4.6 Evaluation of the Influence of Structure on Protein Coverage

A general overview of the structural differences in the three proteins studied is warranted for interpretation of their surface coverage. Lysozyme is a small (MW ≈ 14 kD), rigid protein. For example, it has been demonstrated that LYS maintains its rigid native structure upon adsorption to different surfaces [58]. Bovine IgG has a Y-shaped structure with molecular weight of 150 kD. The IgG molecule is known to adopt orientations ranging between end-on and side-on and it usually adsorbs only through non-specific interaction to the amine-modified substrates [21, 59, 60]. Fibrinogen is a very large (MW = 340 kD), dimeric protein with multiple charge making it very surface active. Given the differences in structure and the heterogeneous nature of protein surfaces generally, these proteins are expected to exhibit different adsorption characteristics on different surfaces.

Figures 9A and 9B respectively show IRRAS spectra following 1 h adsorption of 14.7 and 588 nM solutions of lysozyme (LYS), HFG and bovine IgG onto AUT modified gold substrates. Observance of amide bands in these

three spectra proves that the proteins are indeed adsorbed on AUT self-assembled monolayers. Table 6 presents the summary of infrared spectroscopic measurements of amide bands in Figures 9A and 9B. There are small, but measurable, differences in both amide I and II peak positions for adsorbed proteins. The surface coverage of the proteins for the concentrations studied is given in Table 6. As mentioned earlier, amide II absorbance was used as diagnostic for the amount of protein adsorbed on the AUT-modified gold substrates. An increase in the absorbance of the amide II band is noted for all the proteins in Figure 9B. This increase in the amide II intensity corresponds to an increase in the amount of protein adsorbed to the surface. Lysozyme is the smallest protein therefore recorded the lowest amide II band intensity for both concentrations. In contrast, fibrinogen showed the highest surface coverage (amide II intensity) among the three proteins by virtue of its molecular weight. The non-specifically adsorbed bovine IgG also showed substantially high surface coverage. These outcomes suggest that, the amount of adsorbed protein to surface results from combined effects of surface chemistry, protein structure and lateral interactions between the adsorbed protein molecules.

5. Conclusion

The work presented in this study has demonstrated that FTIR is well suited for exploring the rich chemistries of alkane thiols as well as tracking the surface coverage of adsorbed proteins. Characterization of monolayers using IRRAS made it possible to examine the varied surface chemistries employed. Polystyrene surfaces showed exposed adsorption sites after protein adsorption at both high and low protein concentrations. The use of both direct SAM modified and pre-formed protein substrates provided further insight into the interaction between an adsorbed protein molecule and its solution species. In addition, Langmuir-type isotherms helped in a measure of the binding strength of the adsorbed protein. Coverage of fibrinogen changed according to the surface chemistry and molecular weight of the adsorbed protein. The overall conclusion from the results presented in this manuscript is that surface coverage of an adsorbed protein depends largely on the nature of the substrate and the protein structure.

6. Limitations of the study

The work presented herein is limited to adsorption characteristics of proteins immobilized of solid substrates but not investigation into molecular processes of adsorbed proteins.

7. Recommendations

Further investigation on the secondary structural analysis or at least comparison of normalized amide I bands and comparison with correctly folded protein in solution might be necessary to provide give new information which could be useful for biological/clinical applications.

References

[1] T.A. Horbett, J.L. Brash, Proteins at Interfaces: Current Issues and Future Prospects, in: T.A. Horbett, J.L. Brash (Eds.) ACS Symposium Series 343, American Chemical Society, Washington, DC, Anaheim, CA, 1987, pp. 1-33.

[2] W. Norde, J.G.E.M. Fraaye, J. Lyklema, Acs Symposium Series, 343 (1987) 36-47.

[3] W. Norde, F. Macritchie, G. Nowicka, J. Lyklema, Journal of Colloid and Interface Science, 112 (1986) 447-456.

[4] D.R. Lu, K. Park, Journal of Colloid and Interface Science, 144 (1991) 271-281.

[5] W. Norde, C.E. Giacomelli, Macromolecular Symposia, 145 (1999) 125-136.

[6] M. Matsuda, S. Shiratori, Langmuir, 27 (2011) 4271–4277.

[7] D.J. Vanderah, R.J. Vierling, M.L. Walker, Langmuir, 25 (2009) 5026-5030.

[8] E.P. Vieira, S. Rocha, C.M. Pereira, H. Mohwald, M.A.N. Coelho, Langmuir, 25 (2009) 9879-9886.

[9] M. Matsuda, S. Shiratori, Langmuir, 27 (2011) 4271-4277.

[10] R.J. Hamers, C. Stavis, A. Pokhrel, R. Frankling, R.E. Ruther, X. Wang, M.C. Cooperrider, H. Zheng, J.A. Carlisle, J.E. Butler, Diamond and Related Materials, 20 (2011) 733-742.

[11] R.B. Pernites, C.M. Santos, M. Maldinado, R.R. Ponnapati, D.F. Rodrigues, R.C. Advincula, Chemistry of Materials, 24 (2012) 870-880.

[12] T. Wei, S. Kaewtathip, K. Shing, J. Phys. Chem. C., 113 (2009) 2053-2062.

[13] M.M. Santore, C.F. Wertz, Langmuir, 21 (2005) 10172-10178.

[14] L. Feng, J.D. Andrade, in: T.A. Horbett, J.L. Brash (Eds.) ACS Symposium Series, American Chemical Society, Washington, DC, San Diego, California, 1995, pp. 67-79.

[15] P. Roach, D. Farrar, C.C. Perry, Journal of the American Chemical Society, 128 (2006) 3939-3945.

[16] D. Kiaei, A.S. Hoffman, T.A. Horbett, in: Proteins at Interfaces Ii, 1995, pp. 450-462.

[17] T. Arai, W. Norde, Colloids and Surfaces, 51 (1990) 1-15.

[18] D.J. Vanderah, R.J. Vierling, M.L. Walker, Langmuir 25 (2009) 5026–5030.

[19] C.J. Nonckreman, S. Fleith, P.G. Rouxhet, C.C. Dupont-Gillain, Colloids and Surfaces B: Biointerfaces, 77 (2010) 139–149.

[20] W. Norde, C.A. Haynes, Proteins at Interfaces Ii, 602 (1995) 26-40.

[21] J. Buijs, P.A.W. vandenBerg, J.W.T. Lichtenbelt, W. Norde, J. Lyklema, Journal of Colloid and Interface Science, 178 (1996) 594-605.

[22] J.N. Lin, B. Drake, A.S. Lea, P.K. Hansma, J.D. Andrade, Langmuir, 6 (1990) 509-511.

[23] T.C. Ta, M.T. Sykes, M.T. McDermott, Langmuir, 14 (1998) 2435-2443.

[24] P.S. Sit, R.E. Marchant, Thrombosis and Haemostasis, 82 (1999) 1053-1060.

[25] R.J. Green, R.A. Frazier, K.M. Shakesheff, M.C. Davies, C.J. Roberts, S.J.B. Tendler, Biomaterials, 21 (2000) 1823-1835.

[26] A. Ulman, An Introduction to Ultrathin Organic Films: From Langmuir-Blogett to Self-Assembly, Academic Press Inc., New York, USA, 1991.

[27] R.J. Hamers, C. Stavis, A. Pokhrel, R. Franking, R.E. Ruther, X. Wang, M.C. Cooperrider, H. Zheng, J.A. Carlisle, J.E. Butler, Diamond & Related Materials, 20 (2011) 733–742.

[28] P.S. Sit, R.E. Marchant, Surface Science, 491 (2001) 421-432.

[29] J.E. Puskas, Y. Dahman, A. Margaritis, Biomacromolecules, 5 (2004) 1412-1421.

[30] S. Tunc, M.F. Maitz, G. Steiner, L. Vazquez, M.T. Pham, R. Salzer, Colloids and Surfaces B-Biointerfaces, 42 (2005) 219-225.

[31] A. Naidja, C. Liu, P.M. Huang, Journal of Colloid and Interface Science, 251 (2002) 46-56.

[32] T.C. Ta, M.T. McDermott, Analytical Chemistry, 72 (2000) 2627-2634.

[33] B. Liedberg, B. Ivarsson, P.O. Hegg, I. Lundstrom, Journal of Colloid and Interface Science, 114 (1986) 386-397.

[34] R.E. Marchant, M.D. Barb, J.R. Shainoff, S.J. Eppell, D.L. Wilson, C.A. Siedlecki, Thrombosis and Haemostasis, 77 (1997) 1048-1051.

[35] K.M. Evans-Nguyen, L.R. Tolles, O.V. Gorkun, S.T. Lord, M.H. Schoenfisch, Biochemistry, 44 (2005) 15561-15568.

[36] C.F. Wertz, M.M. Santore, Langmuir, 18 (2002) 706-715.

[37] S.S. Cheng, K.K. Chittur, C.N. Sukenik, L.A. Culp, K. Lewandowska, Journal of Colloid and Interface Science, 162 (1994) 135-143.

[38] C.F. Wertz, M.M. Santore, Langmuir, 15 (1999) 8884-8894.

[39] L.B. Koh, I. Rodriguezb, S.S. Venkatraman, Phys. Chem. Chem. Phys., 12 (2010) 10301–10308.

[40] F. Nsiah, in: Deparment of Chemistry, University of Alberta, Edmonton, 2003, pp. 99.

[41] Q. Yang, Y. Zhang, M. Liu, M. Ye, Y. Zhang, S. Yao, Analytica Chimica Acta, 597 (2007) 58–66.

[42] J.L. Bohnert, T.A. Horbett, Journal of Colloid and Interface Science, 111 (1986) 363-378.

[43] S. Servagent-Noinville, M. Revault, H. Quiquampoix, M.H. Baron, Journal of Colloid and Interface Science, 221 (2000) 273-283.

[44] M.D. Porter, T.B. Bright, D.L. Allara, C.E.D. Chidsey, Journal of the American Chemical Society, 109 (1987) 3559-3568.

[45] R.G. Snyder, M. Maroncelli, H.L. Strauss, V.M. Hallmark, Journal of Physical Chemistry, 90 (1986) 5623-5630.

[46] M. Maroncelli, S.P. Qi, H.L. Strauss, R.G. Snyder, Journal of the American Chemical Society, 104 (1982) 6237-6247.

[47] Z. Pei, L. Busenlehner, S.D. Worley, Y. Tang, C.W. Curtis, Journal of Physical Chemistry B, 101 (1997) 10450-10454.

[48] B. Liedberg, B. Ivarsson, I. Lundstrom, W.R. Salaneck, Progress in Colloid and Polymer Science, 70 (1985) 67-75.

[49] B. Liedberg, B. Ivarsson, I. Lundstrom, Journal of Biochemical and Biophysical Methods, 9 (1984) 233-243.

[50] R. Barbucci, A. Magnani, Biomaterials, 15 (1994) 955-962.

[51] C.E. Giacomelli, M.G.E.G. Bremer, W. Norde, Journal of Colloid and Interface Science, 220 (1999) 13-23.

[52] K.L. Prime, G.M. Whitesides, Science, 252 (1991) 1164-1167.

[53] T.A. Horbett, J.L. Brash, Acs Symposium Series, 343 (1987) 1-33.

[54] D. Kiaei, A.S. Hoffman, T.A. Horbett, K.R. Lew, Journal of Biomedical Materials Research, 29 (1995) 729-739.

[55] S. Oscarsson, Journal of Colloid and Interface Science, 165 (1994) 402-410.

[56] K. Imamura, Y. Kawasaki, T. Awadzu, T. Sakiyama, K. Nakanishi, Journal of Colloid and Interface Science, 267 (2003) 294-301.

[57] R.L. Rich, D.G. Myszka, Journal of Molecular Recognition, 16 (2003) 351-382.

[58] T.J. Su, R.J. Green, Y. Wang, E.F. Murphy, J.R. Lu, R. Ivkov, S.K. Satija, Langmuir, 16 (2000) 4999-5007.

[59] J. Buijs, J.W.T. Lichtenbelt, W. Norde, J. Lyklema, Colloids and Surfaces B-Biointerfaces, 5 (1995) 11-23.

[60] S.F. Chen, L.Y. Liu, J. Zhou, S.Y. Jiang, Langmuir, 19 (2003) 2859-2864.